Int. J. Solids Structures, 1967, Vol. 3, pp. 445 to 470. Pergamon Press Ltd. Printed in Great Britain

ON THE STABILITY OF ECCENTRICALLY STIFFENED CYLINDRICAL SHELLS UNDER AXIAL COMPRESSION*

J. SINGER, M. BARUCH and O. HARARI

Department of Aeronautical Engineering
Technion–Israel Institute of Technology, Haifa, Israel

Abstract—The effect of stiffener eccentricity on the critical load is studied for cylindrical shells under axial compression. Classical simple support and classical clamped end conditions are considered. A detailed physical explanation of the causes of the eccentricity effect is proposed and verified by computations for 350 typical shells.

As in the case of buckling under hydrostatic pressure and torsion, the behavior of the eccentricity effect in the case of axial compression also depends very strongly on the geometry of the shell, represented by the Batdorf parameter. On the other hand the geometry of the stiffeners influences only its magnitude. At very low Z, inversion of the eccentricity effect occurs, but for practical dimensions outside stringers always stiffen the shell more than inside ones. The eccentricity effect has a pronounced maximum at practical values of Z. The behavior of the eccentricity effect is very similar for clamped and for simply supported shells. The effects of eccentricity of ring stiffeners are also considered.

NOTATION

A_n, B_n, C_n	coefficient of displacements
A_1, A_2	cross-sectional area of stringer and ring, respectively
a, b	distance between rings and stringers, respectively
a_q, b_q	defined by equation (15)
D	$[Eh^3/12(1-\nu^2)]$
D_{0q}, D_{1q}, D_{2q}	defined by equation (16)
E, E_1, E_2	moduli of elasticity of shell, stringer and frames, respectively
e_1, e_2	distance between centroid of stiffener cross-section and middle surface shell, positive when inside (see Fig. 1)
$F(q)$	defined by equation (17)
G_1, G_2	shear moduli of stringers and frames, respectively
h	thickness of shell
I_{11}, I_{22}	moment of inertia of stiffener cross-section about its centroidal axis
I_{01}, I_{02}	moment of inertia of stiffener cross-section about the middle surface of the shell
$I_{t1}\ I_{t2}$	torsion constant of stiffener cross-section
L	length of shell between bulkheads
$M_x, M_\phi, M_{x\phi}$	moment resultants acting on element
$\overline{M}_x$	geometrical bending stiffness of stringer–shell combination
m	integer
$N_x, N_\phi, N_{x\phi}$	membrane force resultants acting on element
n	number of half longitudinal waves
$N_{x0}, N_{\phi 0}, N_{x\phi 0}$	prebuckling membrane force resultants
p	hydrostatic pressure
P	axial load
$\overline{P}$	buckling load of equivalently thickened shell computed with empirical buckling coefficients
P_{UNS}	buckling load for unstiffened shell
$P_{\text{UNS. EQ.}}$	buckling load of equivalently thickened shell

* The research reported here was sponsored by the Air Force of Scientific Research OAR under Grant AF EOAR 63–58 through the European Office of Aerospace Research, United States Air Force.

P_{cor}	buckling load of monocoque cylinders corrected by empirical coefficients
q	$(n-1)$ or $(n+1)$
R	radius of shell
t	number of circumferential waves
u^*, v^*, w^*	displacements (see Fig. 1)
u, v, w	non-dimensional displacements ($= u^*/R; v^*/R; w^*/R$ respectively)
x^*, z^*, ϕ	co-ordinates (see Fig. 1)
x, z	non-dimensional co-ordinates ($= x^*/R; z/R$)
Z	$(1-\nu^2)^{\frac{1}{2}}(L/R)^2(R/h)$
$\bar{z}_1$	distance of the centroid of the stringer–shell combination from the middle surface (see Fig. 2)
β	$\pi R/L$
δ_{ij}	$\delta_{ij}+\delta_{0j}$ where δ_{ij} is the Kronecker delta
$\gamma_{x\phi}$	$u_{,\phi}+v_{,x}$
ε_x	$u_{,x}$ } middle surface strains
ε_ϕ	$v_{,\phi}-w$
ζ_1	$(E_1A_1e_1R/hD)$
ζ_2	$(E_2A_2e_2R/aD)$
η_{01}	(E_1I_{01}/bD)
η_{02}	(E_2I_{02}/aD)
η_{t1}	(G_1I_{t1}/bD)
η_{t2}	(G_2I_{t2}/aD)
κ_x	$w_{,xx}$
κ_ϕ	$w_{,\phi\phi}$ } non-dimensional changes of curvature and twist of the middle surface
$\kappa_{x\phi}$	$w_{,x\phi}$
λ	$PR/\pi D$ (when written with the superscript + or − it means axial load parameter for inside or outside stiffened shell)
λ_{UNS}	λ for unstiffened shell
λ_p	$(R^3/D)p$
μ_1	$(1-\nu^2)(E_1A_1/Ebh)$
μ_2	$(1-\nu^2)(E_2A_2/Eah)$
ν	Poisson's ratio
χ_1	$(1-\nu^2)(E_1A_1e_1/EbhR)$
χ_2	$(1-\nu^2)(E_2A_2e_2/EahR)$

Subscripts following a comma indicate differentiation.

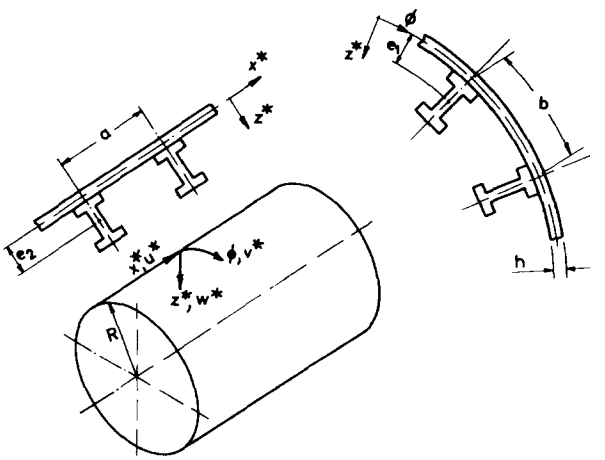

FIG. 1. Notation.

INTRODUCTION

IN 1947 van der Neut [1] showed, for case of buckling under axial compression, that the eccentricity of stiffeners with respect to the skin has great importance. Later in some analyses

of bending and buckling under external pressure, [2–4], the effect of eccentricity was taken into account, but the importance of placing the stiffeners on the inside or outside of the shell for external pressure loading was only recently emphasized [5]. The simple method of analysis of [5] has also been employed for the analyses of stiffened conical shells under hydrostatic pressure, [6] and [7].

Experimental evidence of the importance of the eccentricity of stiffeners was first given by tests carried out at the College of Aeronautics, Cranfield [8] and more recently by the spectacular results of tests at the NASA Langley Research Center [9] and of tests performed by the Lockheed Missiles and Space Company [10]. Further recent experimental evidence can be found in tests carried out at the DFL in Germany [11] on Mylar cylinders.

Recently, many investigators have studied analytically the effect of eccentricity of stiffeners on the buckling of cylindrical shells, especially for the case of axial compression [12] to [18] and [10], and a partial physical explanation of the effect in stringer stiffened shells has recently been given by Thielemann and Esslinger [19]. However, in view of the inversion of the eccentricity effect, first noted in stiffened conical shells under hydrostatic pressure [7] and later in cylindrical shells [15], [17], [20] and [21], a closer look at the effect in axially compressed shells is warranted. In [20] a more complete physical explanation of the eccentricity effect for ring and stringer stiffened shells under external pressure was presented and the physical arguments were verified by extensive calculations, covering a wide range of shell and stiffener geometries. A similar approach is adopted here. A detailed physical explanation of the phenomena is given and then the numerical results are analysed in the light of the expected physical behavior. The eccentricity effect is again shown to be the result of the interplay of two opposing contributions. Inversion of the eccentricity effect is therefore possible also in axially compressed shells, but here it occurs only for extremely short shells which have no practical application. Again, the behavior of the eccentricity effect depends very strongly on the geometry of the shell, while the geometry of the stiffeners only influences its magnitude.

The analysis is an extension of that presented in [5]. However, since here axisymmetric buckling may also be important, the axisymmetric case is added. The analysis of [5] is then extended to clamped cylindrical shells in order to study the effect of rotational restraint at the boundaries on the eccentricity effect. Classical clamped ends, as given for example in [22] are considered. In view of recent work on the effect of the "secondary" boundary conditions on the buckling load of unstiffened cylindrical shells (see for example [23–25]), consideration of only 2 of the 8 possible end conditions may seem incomplete. However, from a recent study of the effect of boundary conditions on the buckling of orthotropic cylindrical shells [26], it appears that the effect of the secondary boundary conditions may be less pronounced in stiffened shells than in unstiffened ones, whereas restraint of end rotations is more important in stiffened shells. The comparison between classical simple supports and clamped ends is therefore significant. After this paper was completed, another of the clamped end conditions ($w = w_{,x} = u = v = 0$) was studied by Card and Jones [27]. Their results reconfirm the importance of rotational restraints in stiffened shells.

SIMPLY SUPPORTED SHELLS

For simply supported shells the present analysis for non-axisymmetric buckling is equivalent to that of [5] and [20]. Hence only the main assumptions of the analysis are

given here and then the final results for axial compression are presented. The main assumptions are:

(a) The stiffeners are "distributed" over the whole surface of the shell.
(b) The normal strains $\varepsilon_x(z)$ and $\varepsilon_\phi(z)$ vary linearly in the stiffener as well as in the sheet. The normal strains in the stiffener and in the sheet are equal at their point of contact.
(c) The shear membrane force $N_{x\phi}$ is carried entirely by the sheet.
(d) The torsional rigidity of the stiffener cross section is added to that of the sheet (the actual increase in torsional rigidity is larger than that assumed).

The middle surface of the shell is chosen as reference line and the expressions for forces and moments in terms of displacements are:

$$
\begin{aligned}
N_x &= [Eh/(1-\nu^2)][u_{,x}(1+\mu_1)+\nu(v_{,\phi}-w)-\chi_1 w_{,xx}] \\
N_\phi &= [Eh/(1-\nu^2)][(v_{,\phi}-w)(1+\mu_2)+\nu u_{,x}-\chi_2 w_{,\phi\phi}] \\
N_{x\phi} &= N_{\phi x} = [Eh/2(1+\nu)](u_{,\phi}+v_{,x}) \\
M_x &= -(D/R)[w_{,xx}(1+\eta_{01})+\nu w_{,\phi\phi}-\zeta_1 u_{,x}] \qquad (1) \\
M_\phi &= -(D/R)(w_{,\phi\phi}(1+\eta_{02})+\nu w_{,xx}-\zeta_2(v_{,\phi}-w)] \\
M_{x\phi} &= +(D/R)[(1-\nu)+\eta_{t1}]w_{,x\phi} \\
M_{\phi x} &= -(D/R)[(1-\nu)+\eta_{t2}]w_{,x\phi} \qquad (2)
\end{aligned}
$$

where $\mu_1, \mu_2, \eta_{01}, \eta_{02}, \eta_{t1}$ and η_{t2} are the changes in stiffnesses due to stringers and frames and χ_1, χ_2, ζ_1 and ζ_2 are the changes in stiffnesses caused by the eccentricities of the stringers and rings, as in [5]. Since the analysis is concerned with instability, u, v and w are the additional displacements during buckling, and as in [5] they are non-dimensional, the physical displacements having been divided by the radius of the shell.

The classical simple support boundary conditions

$$
\begin{aligned}
w &= 0 \\
M_x &= 0 \\
N_x &= 0 \\
v &= 0
\end{aligned} \qquad (3)
$$

are assumed and

$$
\begin{aligned}
u &= A_n \sin t\phi \cos n\beta x \\
v &= B_n \cos t\phi \sin n\beta x \qquad (4) \\
w &= C_n \sin t\phi \sin n\beta x
\end{aligned}
$$

are the displacements which solve the Donnell type stability equations for general instability, equation (12) of [5], in the presence of these boundary conditions.

Assuming that the prebuckling stresses are represented satisfactorily by the membrane stresses

$$\begin{aligned} N_{x0} &= -(P/2\pi R) \\ N_{\phi 0} &= 0 \\ N_{x\phi 0} &= 0 \end{aligned} \tag{5}$$

the third stability equation, equation (18) of [5], becomes for the case of axial compression

$$\begin{aligned} &\zeta_1(-n^3\beta^3 a_n)+\zeta_2(-2t^2-b_n t^3)+(1+\eta_{01})n^4\beta^4+(2+\eta_{t1}+\eta_{t2})n^2\beta^2 t^2+(1+\eta_{02})t^4 \\ &+12(R/h)^2[(1+\mu_2)(1+b_n t)+\nu n\beta a_n]-\lambda(n^2\beta^2/2)=0 \end{aligned} \tag{6}$$

where λ is a non-dimensional axial load parameter defined by:

$$\lambda = (PR/\pi D) = [12(1-\nu^2)PR/\pi Eh^3] \tag{7}$$

and a_n and b_n are given by equations (16) of [5].

The integer values of t and n (the circumferential waves and axial half-waves, respectively) which make λ a minimum have to be chosen to yield the critical axial load.

In cylindrical shells subjected to axial compression, axisymmetric buckling may occur under certain conditions. The axisymmetric mode can be obtained from the non-axisymmetric analysis by letting $t = 0$. Then equation (6) becomes

$$\lambda/2 = (1+\eta_{01})n^2\beta^2+[12(R/h)^2/n^2\beta^2]\{1+\mu_2-[(\nu-\chi_1 n^2\beta^2)^2/(1+\mu_1)]\} \tag{8}$$

The integer value of n which makes λ a minimum has to be used in calculations. When the shell is stiffened by rings only, equation (8) simplifies to

$$\lambda = 2\{n^2\beta^2+[12(R/h)^2(1+\mu_2-\nu^2)/n^2\beta^2]\} \tag{9}$$

and if one assumes that there are many waves in the axial direction and that n can be treated as a continuous variable, the critical value of λ becomes

$$\lambda_{\text{crit}} = 8(\sqrt{3})(R/h)\sqrt{(1+\mu_2-\nu^2)} = 8(\sqrt{3})(R/h)\sqrt{\{(1-\nu^2)[1+(A_2/ah)]\}} \tag{10}$$

In [28], equation (8) is also rederived with axisymmetry assumed from the beginning.

CLAMPED SHELLS

The analysis of [5] is now extended to clamped cylindrical shells and is presented for axial compression and hydrostatic pressure. The same assumptions are made as for the simply supported shells, except that the classical clamped boundary conditions

$$\begin{aligned} w &= 0 \\ w_{,x} &= 0 \\ u &= 0 \\ N_{x\phi} &= 0 \end{aligned} \tag{11}$$

are considered instead of equation (3). Displacements similar to those proposed by Batdorf [22] for unstiffened clamped cylindrical shells are assumed here

$$
\begin{aligned}
u &= \sum_{n=1}^{\infty} (1/2)[A_{1n}\sin(n-1)\beta x - A_{2n}\sin(n+1)\beta x]\sin t\phi \\
v &= \sum_{n=1}^{\infty} (1/2)[B_{1n}\cos(n-1)\beta x - B_{2n}\cos(n+1)\beta x]\cos t\phi \\
w &= \sum_{n=1}^{\infty} C_n(1/2)[\cos(n-1)\beta x - \cos(n+1)\beta x]\sin t\phi
\end{aligned}
\tag{12}
$$

When the shell is subjected to both axial compression and hydrostatic pressure the prebuckling stresses are taken as the sum of the membrane stresses, equation (5) of this paper and equations (13) of [5]. The Donnell type stability equations in terms of displacements, equations (12) of [5], are then

$$
\begin{aligned}
&[Eh/(1-\nu^2)]\{(1+\mu_1)u_{,xx} + [(1-\nu)/2]u_{,\phi\phi} + [(1+\nu)/2]v_{,x\phi} - \chi_1 w_{,xxx} - \nu w_{,x}\} = 0 \\
&[Eh/1-\nu^2]\{[(1+\nu)/2]u_{,x\phi} + (1+\mu_2)v_{,\phi\phi} + [(1-\nu)/2]v_{,xx} - (1+\mu_2)w_{,\phi} - \chi_2 w_{,\phi\phi\phi}\} = 0 \\
&(-D/R)\{\zeta_1(-u_{,xxx}) + \zeta_2(2w_{,\phi\phi} - v_{,\phi\phi\phi}) + (1+\eta_{01})w_{,xxxx} + (2+\eta_{t1}+\eta_{t2})w_{,xx\phi\phi} \\
&\quad + (1+\eta_{02})w_{,\phi\phi\phi\phi} + 12(R/h)^2[(1+\mu_2)(w-v_{,\phi}) - \nu u_{,x}] + \lambda(w_{,xx}/2) \\
&\quad + \lambda_p[(w_{,xx}/2) + w_{,\phi\phi}]\} = 0
\end{aligned}
\tag{13}
$$

The first two of the stability equations, equations (13), are solved by the assumed displacements, equation (12), in the same manner as in [5]. The displacements can then be written as

$$
\begin{aligned}
u &= \sum_{n=1}^{\infty} C_n(\tfrac{1}{2})\{-a_{n-1}\sin[(n-1)\beta x] + a_{n+1}\sin[(n+1)\beta x]\}\sin t\phi \\
v &= \sum_{n=1}^{\infty} C_n(\tfrac{1}{2})\{b_{n-1}\cos[(n-1)\beta x] - b_{n+1}\cos[(n+1)\beta x]\}\cos t\phi \\
w &= \sum_{n=1}^{\infty} C_n(\tfrac{1}{2})\{\cos[(n-1)\beta x] - \cos[(n+1)\beta x]\}\sin t\phi
\end{aligned}
\tag{14}
$$

where

$$
\begin{aligned}
a_q &= D_{1q}/D_{0q} \\
b_q &= D_{2q}/D_{0q}
\end{aligned}
\tag{15}
$$

and q represents $(n-1)$ and $(n+1)$ respectively

$$
\begin{aligned}
D_{0q} &= [(1-\nu)/2]\{(1+\mu_2)t^4 + [(1+\mu_1)(1+\mu_2) - \nu]q^2\beta^2t^2 + (1+\mu_1)[(1-\nu)/2]q^4\beta^4 \\
D_{1q} &= -[(1+\nu)/2]\chi_2 q\beta t^4 + (1+\mu_2)\{\chi_1 q^3\beta^3 + [(1-\nu)/2]q\beta\}t^2 \\
&\quad + \chi_1[(1-\nu)/2]q^5\beta^5 - \nu[(1-\nu)/2]q^3\beta^3 \\
D_{2q} &= [(1-\nu)/2]\chi_2 t^5 + \{(1+\mu_1)\chi_2 q^2\beta^2 - [(1-\nu)/2](1+\mu_2)\}t^3 \\
&\quad + \left\{\{[(1+\nu)/2]\nu - (1+\mu_1)(1+\mu_2)\}q^2\beta^2 - [(1+\nu)/2]\chi_1 q^4\beta^4\right\}t
\end{aligned}
\tag{16}
$$

Note that D_{0q}, D_{1q} and D_{2q} when $q = n$ are identical to D_{0n}, D_{1n} and D_{2n} given by equations (17) of [5].

Here, however, the third of the stability equations (13), cannot be solved in closed form and hence it is solved by the Galerkin method. If one defines

$$F(q) = \zeta_1(-q^3\beta^3 a_q)+\zeta_2(-2t^2-b_q t^3)+(1+\eta_{01})q^4\beta^4+(2+\eta_{t1}+\eta_{t2})q^2\beta^2t^2+(1+\eta_{02})t^4 + 12(R/h)^2[(1+\mu_2)(1+b_q t)+\nu q\beta a_q]-\lambda(q^2\beta^2/2)-\lambda_p[(q^2\beta^2/2)+t^2] \tag{17}$$

the Galerkin integrals, for an N term solution, yield a set of N algebraic equations

$$\sum_{n=1}^{N} C_n\{F(n-1)[\bar{\delta}_{(n-1)(m-1)}-\bar{\delta}_{(n-1)(m+1)}]-F(n+1)[\bar{\delta}_{(n+1)(m-1)}-\bar{\delta}_{(n+1)(m+1)}]\} = 0 \tag{18}$$

$$m = 1, 2, \ldots, N$$

where

$$\bar{\delta}_{ij} = \delta_{ij}+\delta_{0j} \tag{19}$$

and δ_{ij} is the Kronecker delta defined by

$$\begin{aligned} \delta_{ij} &= 0 \quad \text{when} \quad i \neq j \\ \delta_{ij} &= 1 \quad \text{when} \quad i = j \end{aligned} \tag{20}$$

The determinant of the coefficients of C_n in equations (18), the stability determinant, can be resolved into two subdeterminants, one of the even components and one of the odd components representing symmetric and antisymmetric buckling modes. The symmetric buckling pattern is hence represented by $n = 1, 3, 5, \ldots$ and $m = 1, 3, 5, \ldots$ and the antisymmetric buckling pattern by $n = 2, 4, 6, \ldots$ and $m = 2, 4, 6, \ldots$.

The critical load has to be computed for both buckling patterns. However, the numerical work indicates that the antisymmetric mode usually yields higher buckling loads except for very long and thin shells.

PHYSICAL EXPLANATION

A physical explanation of the effect of eccentricity of rings on the instability of stiffened cylindrical shells under hydrostatic pressure is given in [20]. There, the explanation is given for rings because rings are most effective in stiffening against hydrostatic pressure. For axial compression stringers are much more effective than rings and therefore the effect of the eccentricity of stringers will be considered here in detail.

The explanation follows the lines of that given in [20], but there are important differences between the behavior of stringer–stiffened shells under axial compression and that of ring-stiffened shells under hydrostatic pressure.

The total geometrical bending stiffness of the combined stringer–shell cross-section is not affected by the position of the stringers and is equal for outside and inside stringers. (Actually, the moment of inertia of the combined stringer–shell cross-section is larger for outside stringers but for closely spaced stringers this difference is small and can be neglected. When the closely spaced stringers are "distributed" there is no difference at all.) As a result of the initial curvature of the shell, additional membrane forces appear in it during

buckling. If one considers the circumferential membrane forces, this is immediately apparent, since for outward buckles the shell has to lengthen and tensile forces arise, while for inward buckles the shell has to shorten and compressive forces arise.

A relation between the axial and circumferential membrane forces is obtained by differentiation of the first two stability equations (equations (11) of [5] or equations (4) of [20]) with respect to x and ϕ, which yields

$$N_{x,xx} = N_{\phi,\phi\phi} \tag{21}$$

By substitution of the assumed displacements for simple supports, equations (4), into equation (21) this relation between the membrane forces becomes

$$n^2\beta^2 N_x = t^2 N_\phi \tag{22}$$

As mentioned, N_ϕ is compressive in a positive (inward) wave and tensile in a negative wave. From equation (22) it is seen that N_x follows N_ϕ at every point of the shell.

It should be noted that equation (22) applies to the classical simple support boundary conditions, equations (3). For the classical clamped boundary conditions, equation (11), a similar relation between N_x and N_ϕ can be obtained when $n = 1$, since substitution of equation (14) into equation (21), with $n = 1$, yields

$$(n+1)^2\beta^2 N_x = 4\beta^2 N_x = t^2 N_\phi \tag{23}$$

For $n \neq 1$ the relation cannot be expressed in such a simple manner, though it is similar in character. However, heavily stiffened cylindrical shells of practical dimensions tend to buckle with $n = 1$, unless they are very long. For long shells, the buckling pattern repeats itself, and though n increases, β decreases simultaneously with the result that $n\beta$, which is really the important quantity in equations (22) and (23), remains nearly constant. Hence the conclusions drawn from equation (22) apply approximately also to classical clamped ends, and may be expected to apply approximately also to the other boundary conditions not considered here.

In Figs. 2(a) to 2(d), $\bar{M}_x$ represents the geometrical bending stiffness of the cross-section of the stringer–shell combination. $\bar{M}_x$ is the moment necessary to produce a certain change in curvature and is equal for inside and outside stringers. However, due to the longitudinal membrane force acting in the shell, the actual total bending stiffness of the cross-section is changed. For a stringer–shell combination with inside stringers the actual total bending stiffness is [see Figs. 2(a) and 2(c)]

$$M_x^{\text{in}} = \bar{M}_x - \bar{z}_1 N_x^{\text{in}} \tag{24}$$

where M_x^{in} is the actual moment necessary to produce the same change of curvature that $\bar{M}_x$ would produce without the membrane force N_x^{in}.

In the same manner, the actual bending stiffness for the cross-section with outside stringers is [see Figs. 2(b) and 2(d)]

$$M_x^{\text{out}} = \bar{M}_x + \bar{z}_1 N_x^{\text{out}} \tag{25}$$

where again M_x^{out} is the actual moment necessary to produce the same change of curvature which $\bar{M}_x$ would produce without the membrane force N_x^{out}.

From equations (24) and (25) it can be seen that the actual bending stiffness for outside stiffening is larger than that for inside stiffening. This is the primary eccentricity effect.

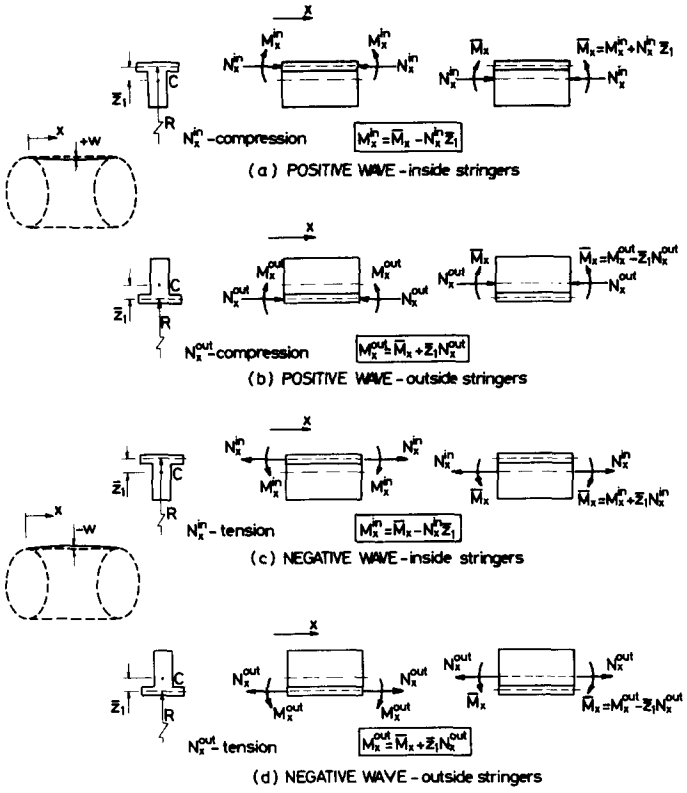

FIG. 2. The primary eccentricity effect.

There is, however, another opposing secondary effect that influences the behavior of the eccentrically stringer-stiffened shells under axial compression, though its influence is less noticeable here than for ring-stiffened shells under hydrostatic pressure.

Consider a shell with inside stringers. In a positive wave, the moment M_x produces in the shell an additional compressive strain in the longitudinal direction. Due to Poisson's effect (ν), a circumferential strain appears in the sheet, giving rise to an additional compressive membrane force, ΔN_ϕ, in the circumferential direction, which resists this strain. This additional compressive membrane force has a radial component which resists radial deformation [Fig. 3(a)]. On the other hand, for outside stringers the additional force ΔN_ϕ is tensile and therefore assists deformation [Fig. 3(b)]. In a negative wave [Figs. 3(c) and 3(d)] the same argument applies and the additional membrane force, ΔN_ϕ, resists the deformation for inside stringers, whereas it assists it for outside stringers.

The effect of eccentricity of stringers can therefore be summarized as follows:

1. *Primary effect*—outside stringers increase the actual bending stiffness in the longitudinal direction more than inside stringers.
2. *Secondary effect*—inside stringers increase the actual extensional stiffness in the circumferential direction more than outside stringers.

Now, for short cylinders the main resistance to buckling is in the longitudinal direction. M_x is the main component of the resistance of the shell. N_x is very small and therefore the

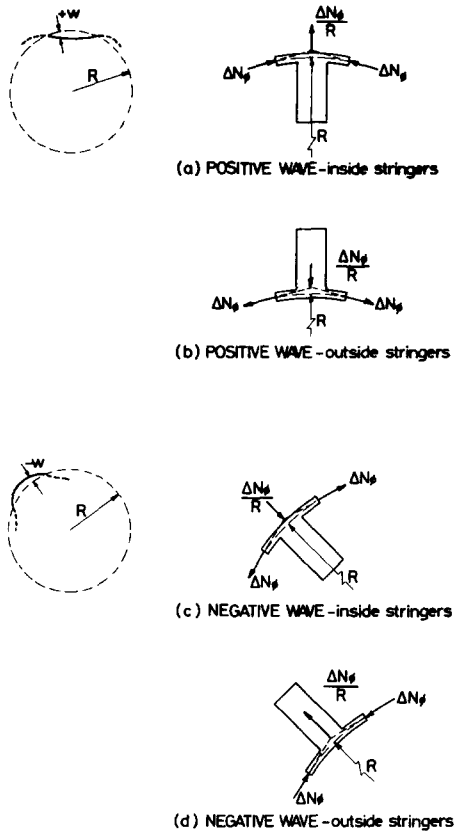

FIG. 3. The secondary eccentricity effect.

difference in the actual bending stiffness for inside and outside stringers is also small. Since M_x is large and the secondary effect is important for very short cylinders, inside stringers may yield larger critical axial loads than outside stringers, as is indeed found in the computations. It should be remembered that the secondary effect depends entirely on Poisson's ratio ν. Variation of ν will therefore noticeably influence the secondary effect. With $\nu = 0{\cdot}5$ the secondary effect is enhanced while with $\nu = 0$ it vanishes, as is later verified in the numerical work.

For medium length cylinders M_x is still important, but N_x increases and therefore the difference between the actual longitudinal bending stiffnesses for outside and inside stringers also increases. Hence the critical axial load is much larger with stringers on the outside than on the inside of the shell.

For long cylinders, the difference between the actual longitudinal bending stiffnesses for outside and inside stringers continues to increase. The contribution of the membrane force to the actual total bending stiffness, $\bar{z}_1 N_x$, becomes larger than M_x and for inside stringers the actual bending stiffness, M_x^{in}, may even change sign and become negative. This has been verified for a typical long shell.

However, the total difference between the critical axial load for outside and inside stringers decreases as the length of the shell increases, or more precisely, as Z increases.

This is caused by the diminishing relative importance of M_x and N_x in resisting buckling for long shells, in which M_ϕ is the main element of buckling strength of the shell. Since M_ϕ is not affected by the eccentricity of the stringers, the total eccentricity effect declines in long shells.

Rings are much less effective than stringers in stiffening of cylindrical shells subjected to axial compression, when alone. However, they may increase the buckling load considerably when they act together with stringers, see Section 3 of [29]. Furthermore, the behavior of ring stiffened shells under axial compression is also of interest since shells primarily designed to withstand lateral pressure (which will be predominantly ring stiffened) may be subjected to axial loads under certain conditions.

The eccentricity effect of rings in an axially compressed cylindrical shell is basically the same as that considered above for stringers and given in detail for ring stiffened shells subjected to hydrostatic pressure in [20]. The same primary and opposing secondary effects could be discerned and ranges should occur where the primary effect dominates and outside rings yield higher loads than inside rings, and where the secondary effect dominates and inside rings are better. However, under axial compression ring stiffened shells buckle with many longitudinal waves, unless the shell is very short, and hence subdivide into many short "bays". As a result, the axially compressed ring-stiffened shell is always in the "short shell" range where outside rings should yield higher buckling loads than inside ones. The computations verify this argument.

The discussion up to this point has only considered non-axisymmetric buckling patterns, and the possibility of axisymmetric buckling has now to be considered. Since in the axisymmetric buckling pattern no bending occurs in the circumferential direction, the eccentricity of rings cannot affect the critical load when the shell buckles in this mode. This is verified by the axisymmetric analysis, see equation (8), where no terms containing the eccentricity of rings appear. Only the added area of the ring stiffens the shell against circumferential extension and compression, but this stiffening is the same for outside and inside rings.

One should now remember that for isotropic cylindrical shells under axial compression the classical buckling load is the same for axisymmetric and non-axisymmetric buckling, provided $n\beta$ and t (the longitudinal wave parameter and the number of circumferential waves) are large enough to be considered continuous, or is approximately the same otherwise, see for example [30]. From an energy point of view this means that the same amount of strain energy is absorbed by a shell buckling in an axisymmetric pattern (sometimes called ring-shape pattern) and by one buckling in a non-axisymmetric pattern (sometimes called chess-board pattern).

For ring-stiffened shells this is no longer so. Consider first centrally placed rings ($e_2 = 0$). As was already found by Thielemann for orthotropic shells [31], the classical linear theory buckling loads, characterized by chess-board (asymmetric) and ring-shape (axisymmetric) buckling, no longer coincide in general. For a ring-stiffened cylindrical shell the chess-board pattern usually yields a slightly lower buckling load than the ring-shape pattern. This may be explained by energy considerations. The cross-sectional area added to the shell by the rings stiffens it considerably against circumferential extension or compression. Axisymmetric buckling, in which most of the strain energy absorbed is the extensional strain energy due to the circumferential extension and compression of the shell, would therefore require appreciably more energy input. On the other hand, in non-axisymmetric buckling only a smaller fraction of the strain energy is absorbed in extensional

deformation and the remainder is due to bending in the longitudinal and circumferential directions. For a hypothetical shell, in which the rings add only cross-sectional area but no increase in moment of inertia in the circumferential direction, the chess-board pattern will obviously yield a lower buckling load than the ring-shape pattern. For, in comparison to an unstiffened shell, the increase in area in the stiffened shell due to the rings affects a smaller portion of the total strain energy in non-axisymmetric buckling than in the axisymmetric pattern. As the moment of inertia of the rings is increased, for constant cross-sectional area, the energy absorbed by circumferential bending increases and the buckling load of the chess-board pattern rises and approaches that for the ring-shape pattern. For fairly large I_{22}, non-axisymmetric buckling would require more energy input than symmetric buckling, and hence above a certain magnitude of I_{22} the shell will always buckle in an axisymmetric pattern. This is verified by computations for a typical shell (see Table 2).

When the rings are eccentrically positioned, outside rings should yield higher buckling loads than inside ones in non-axisymmetric buckling, since axially compressed ring-stiffened shells are always in the "short" shell range. With inside rings, non-axisymmetric buckling will occur and the positive eccentricity will lower the buckling below that for centrally placed rings. With outside rings, however, the increase in buckling load that would result from the negative eccentricity if the shell were to buckle in a chess-board pattern, is not realized, since the shell now buckles in the ring-shape pattern which is unaffected by eccentricity and yields a lower buckling load. In shells with very small negative eccentricity and small I_{22}, chess-board patterns are still possible, but for practical dimensions the axisymmetric buckling mode always predominates in this case. Computations for typical shells verify the arguments presented.

For design purposes, the small differences between axisymmetric and non-axisymmetric buckling for centrally placed or outside rings, discussed above, may be neglected. One can therefore conclude roughly that with inside rings a chess-board pattern occurs and the buckling load is reduced by the eccentricity of the rings, whereas with outside rings the axisymmetric pattern dominates and the magnitude of the eccentricity does not affect the buckling load.

NUMERICAL RESULTS AND DISCUSSION

The critical axial loads have been computed for 350 ring and stringer stiffened shells covering a wide range of shell and stiffener geometries.

The computations were carried out on the Elliot 803 and 503 computers of the Technion Computing Center. The shell geometries considered cover (L/R) from 0·25 to 20·0 and (R/h) from 50 to 50,000, and the stringer geometries include (A_1/bh) from 0·1 to 5·0, (I_{11}/bh^3) from 1·0 to 20·0 and (e_1/h) from 1·0 to 10·0. The ring geometries considered cover a smaller range.

In order to study the behavior of the secondary effect, the variation of the total eccentricity effect, (P^{out}/P^{in}), with Z is plotted for different values of Poisson's ratio in Fig. 4. The extreme values of ν considered, $\nu = 0$ and $\nu = 0{\cdot}5$ are unrealistic, but bring out very clearly the dependence of the secondary effect on ν. With $\nu = 0$ the secondary effect disappears, while with $\nu = 0{\cdot}5$ it is enhanced. For very small values of Z, the curves for $\nu = 0{\cdot}5$ fall below $(P^{out}/P^{in}) = 1$. Hence an inversion of the eccentricity effect is demonstrated. In the range of Z below the inversion point, inside stringers yield higher buckling loads than

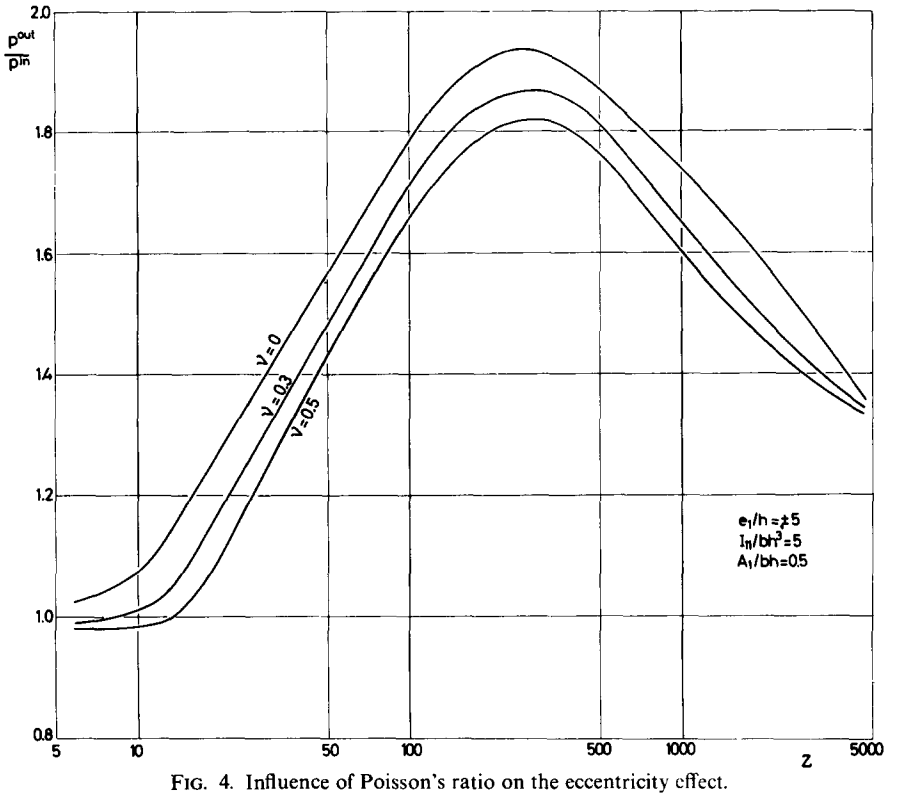

FIG. 4. Influence of Poisson's ratio on the eccentricity effect.

outside ones. There the primary effect is overshadowed by the secondary effect as the result of the growing importance of M_x relative to N_x. For $\nu = 0$ there is no inversion and the curve tends asymptotically (from the positive side) to $(P^{out}/P^{in}) = 1$. This verifies the physical arguments that link the secondary effect to Poisson's ratio.

With increase in Z, the eccentricity effect increases and passes a maximum (which is discussed below), and for large values of Z all the curves merge into one. This indicates that for large Z the primary effect remains the sole contributor to the total eccentricity effect.

In Fig. 5 the curve for $\nu = 0{\cdot}3$ and simple supports is redrawn, but with the computed points to bring out the dominant dependence of the eccentricity effect on the shell geometry. Again, as in [20] and [21], the Batdorf parameter, $Z = (1-\nu^2)^{\frac{1}{2}}(L/R)^2(R/h)$, represents the shell geometry rather well. The scatter of the points about the (P^{out}/P^{in}) curve is mainly caused by the necessary periodicity of the waves in the circumferential direction, which would appear as ripples if the values of P^{out} or P^{in} were plotted versus Z. The curves in Figs. 4 and 5 smooth out the effect of these ripples on the ratio (P^{out}/P^{in}). As Z increases further, the (P^{out}/P^{in}) curve approaches asymptotically a value larger than 1, since in the case of long shells under axial compression the buckling pattern divides the shell into "sub-cylinders" having the same critical load and hence the length ceases to affect the buckling load beyond a certain (L/R).

The maximum which appears in the curves of Figs. 4 and 5 represents a general characteristic behavior of stringer-stiffened cylindrical shells under axial compression that is caused by the primary effect described in the preceding section. The primary effect is

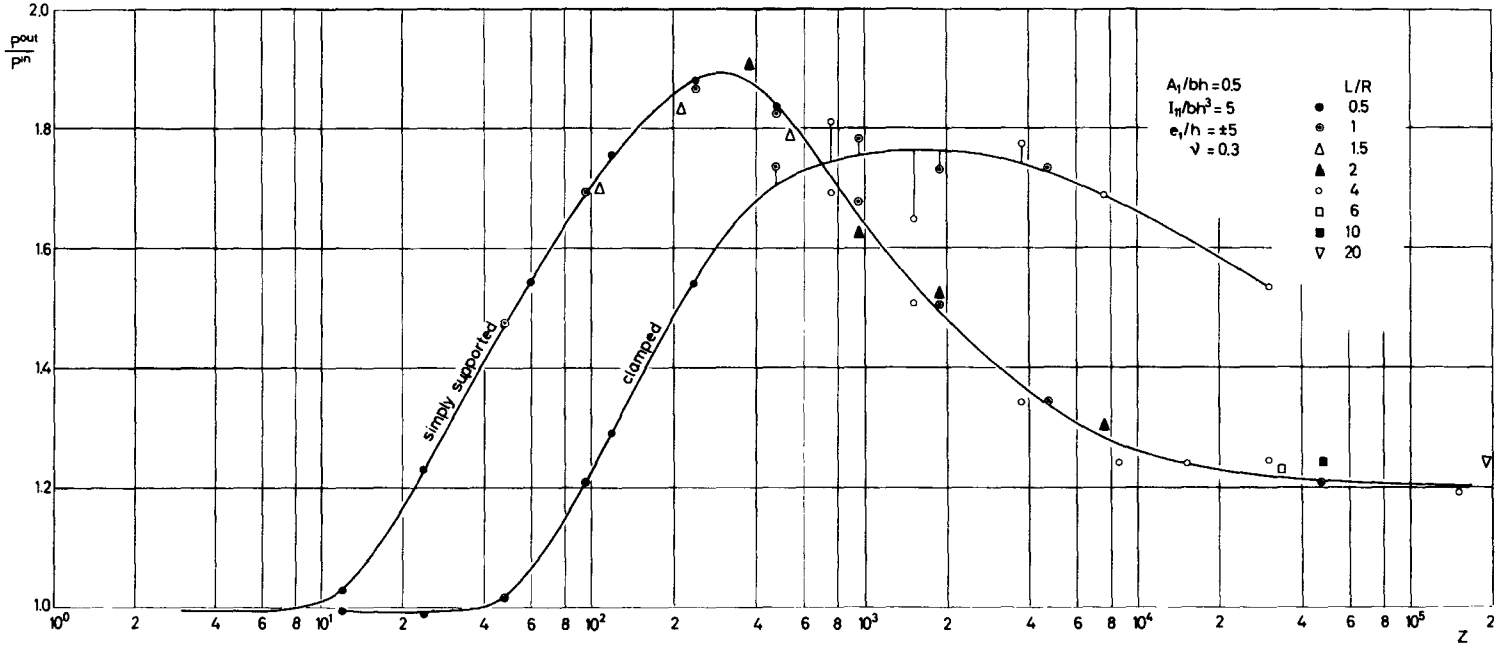

FIG. 5. Variation of eccentricity effect with shell geometry and boundary conditions.

represented there by equations (24) and (25) and depends mainly on the magnitude of the governing factors $N_x\bar{z}_1$ and M_x. The larger $N_x\bar{z}_1$ is as compared to M_x, the more pronounced is the difference between shells with stiffeners on the outside and those with stiffeners on the inside. One could, therefore, expect a monotonous rise of the eccentricity effect with Z, since N_x remains relatively large even for long shells, while M_x (which depends on $w_{,xx}$) decreases rapidly. However, in this discussion only the forces and moments in the axial direction have been considered, whereas actually also circumferential forces and moments contribute to the resistance against buckling. The relative contribution of N_ϕ and even more so of M_ϕ grows as Z increases. But since for a stringer stiffened shell N_ϕ and M_ϕ are practically unaffected by e_1, the rise in (P^{out}/P^{in}) is slowed down by this "neutral" influence as Z increases, and eventually is changed to a decline.

Or, more precisely: up to $Z = 500$, stringers are very effective since they influence N_x and M_x, which predominate in this range of Z. On the other hand, long shells, with large Z, behave approximately as unstiffened shells, and M_ϕ, which is here unaffected by the eccentricity, overshadows the other factors. Between these two extremes there is a range of Z where axial and circumferential forces and moments make similar contributions to the stiffness of the shell. This is the range where the maximum eccentricity effect occurs.

The variation of (P^{out}/P^{in}) with Z is plotted in Fig. 5 also for clamped cylindrical shells, and clamping implies here the classical clamped boundary condition given by equations (11). The behavior of the total eccentricity effect for clamped cylindrical shells is seen to be very similar to that of simply supported shells. (P^{out}/P^{in}) again has a maximum, which, however, is of slightly smaller magnitude than that for simple supports and occurs at a larger Z. The total eccentricity effect also falls off more slowly with Z for the clamped shell than for the simple supported one and outside stringers remain noticeably better than inside ones even at very high values of Z. The scatter of the points about the (P^{out}/P^{in}) curve is wider here than for simple supported shells. In clamped shells the scatter is partly caused by the necessary integer values of the number of circumferential waves, as for simple supports, and partly by the appearance of longitudinal antisymmetric buckling modes. The physical explanation of the eccentricity effect applies also to clamped shells, and indeed the main influence of the clamping of the eccentricity effect seems to be a shifting of the (P^{out}/P^{in}) curve to higher values of Z.

Figure 6 shows the structural efficiencies of eccentrically stiffened shells. For a typical stringer geometry, the ratio of the buckling load of stiffened shells to that of equivalent unstiffened shells is plotted versus Z for outside, inside and centrally placed stringers and for simple supports and clamped ends. Equivalency here implies identical weight. The critical loads of clamped stiffened shells are actually compared with those of equivalent unstiffened shells on simple supports instead of clamped ends. However, except for very low values of Z (not represented in Fig. 6) unstiffened shells with clamped ends have practically the same buckling loads as simply supported ones, see [24], and hence the comparison is valid. Note also that the buckling loads are calculated with linear theory, and hence the values for unstiffened shells are unrealistic. Hence the curves in Fig. 6 are conservative and the actual structural efficiency of stiffened shells is higher than shown in Fig. 6. In Figs. 11 and 12 below, the structural efficiencies of stiffened shells are re-evaluated by comparison with empirical buckling loads of the unstiffened shells.

In the computations, some interesting results were obtained for M_x in shells with inside stiffeners. According to equations (24) and (25), M_x^{out} and M_x^{in} are increased and decreased respectively by the influence of the membrane forces. The validity of equations (24) and

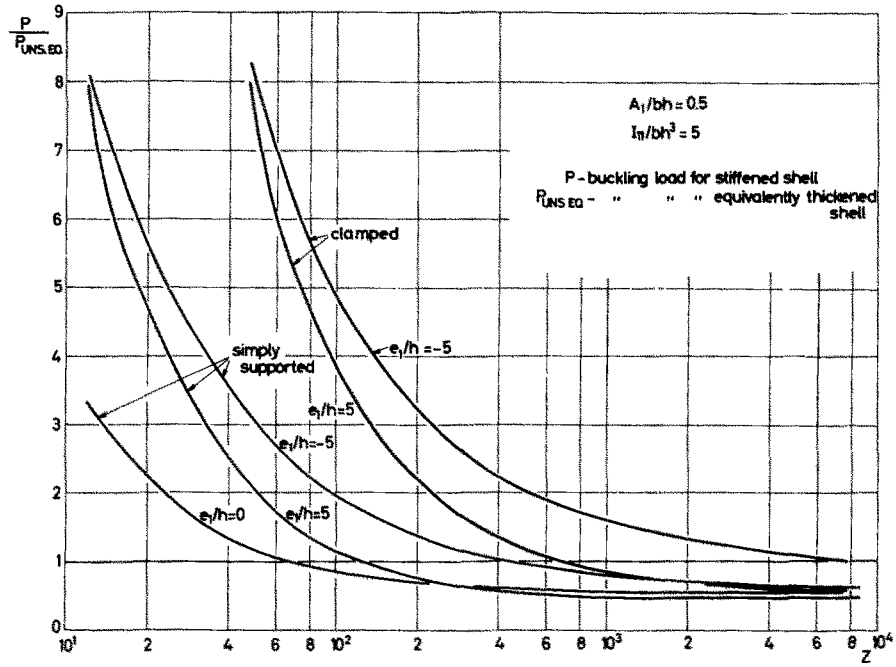

FIG. 6. Effect of end conditions on the structural efficiency of eccentrically stiffened shells.

(25), and the physical explanation they represent, is confirmed by numerical results. In certain cases it was found that M_x is not only decreased for inside stringers but actually changes sign (for example, for the typical shell $(R/h) = 250$, $(L/R) = 4{\cdot}0$, $(A_1/bh) = 0{\cdot}5$, $(e_1/h) = 5$ and $(I_{11}/bh^3) = 5$). This means that, in certain cases, a negative moment M_x has to be applied for a positive curvature of the shell in order to reduce the positive moment contribution of the eccentrically applied membrane forces (see Fig. 2). In the mathematical formulation, equation (2), this change of sign of M_x means that the bending stiffness of the shell-stiffener combination, represented here by $(1+\eta_{01})w_{,xx}$, is overshadowed by the term $-\zeta_1 u_{,x}$ that represents the bending contribution of the membrane forces.

In Fig. 7, the influence of stiffener geometry parameters on the buckling load is investigated for 3 typical shells. The variation of (P^{out}/P_{UNS}) and (P^{in}/P_{UNS}) with magnitude of eccentricity, cross-sectional area and moment of inertia of stringers is plotted, where P_{UNS} is the classical buckling load of the unstiffened shell. Except for very low values of Z, the buckling load is not increased appreciably by variation of (I_{11}/bh^3), (e_1/h) and (A_1/bh). Indeed, in long shells with inside stringers increase of eccentricity, (e_1/h), reduces the buckling load below that of the equivalent orthotropic cylinder, $(e_1/h) = 0$. This behavior can also be observed in Fig. 6, where the curve for $(e_1/h) = 5$ falls below that for $(e_1/h) = 0$ as Z increases beyond 300.

In Figs. 8 and 9, the influence of stringer cross-sectional area A_1 and magnitude of eccentricity e_1 on the eccentricity effect are investigated. The moment of inertia of the stringer about its centroid I_{11} is only a parameter of secondary importance, since it does not influence χ_1 and ζ_1 which determine the eccentricity effect. In all the curves in Figs. 8 and 9 a maximum occurs at almost the same value of Z. Even a radical change in magnitude of eccentricity from $(e_1/h) = 2$ to $(e_1/h) = 10$ causes only a slight shift in the position of the

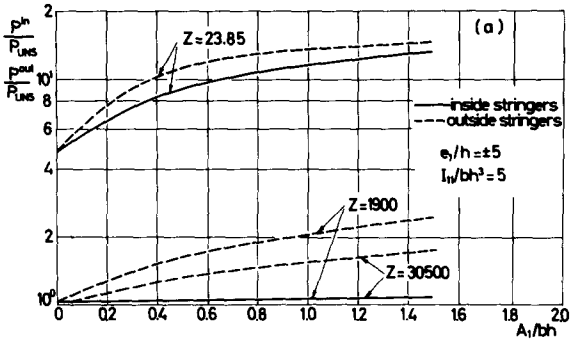

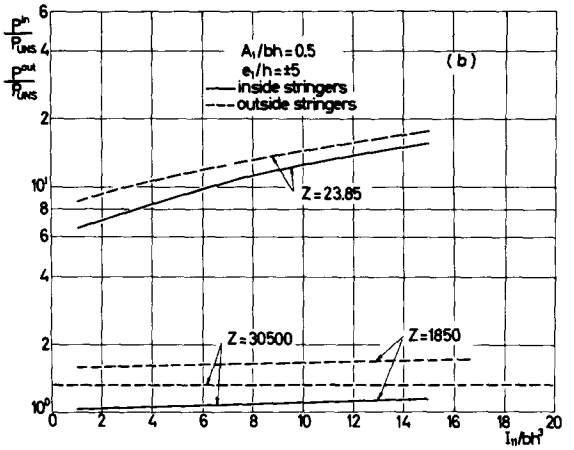

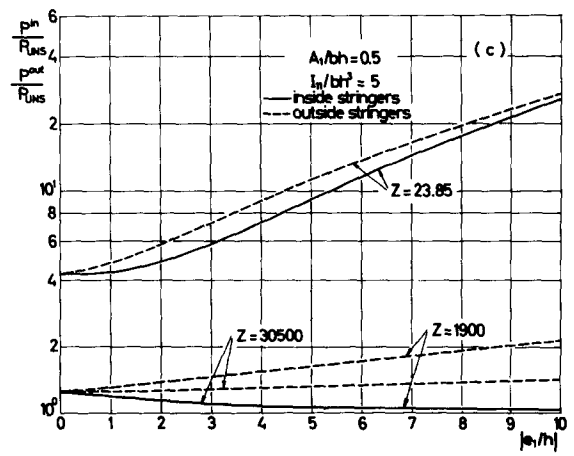

FIG. 7(a,b,c). Effect of stiffener geometry on stiffening of shell.

maximum from $Z = 200$ to $Z = 800$. In very heavily stiffened shells, for example, $(A_1/bh) = 3$ and $(A_1/bh) = 5$ with $(e_1/h) = 10$ in Table 1, differences in buckling load of more than 500% are obtained between outside and inside stringers. Such stringers are not realistic, but they indicate that the (P^{out}/P^{in}) ratio continues, in principle, to rise monotonically with increasing stiffener rigidity.

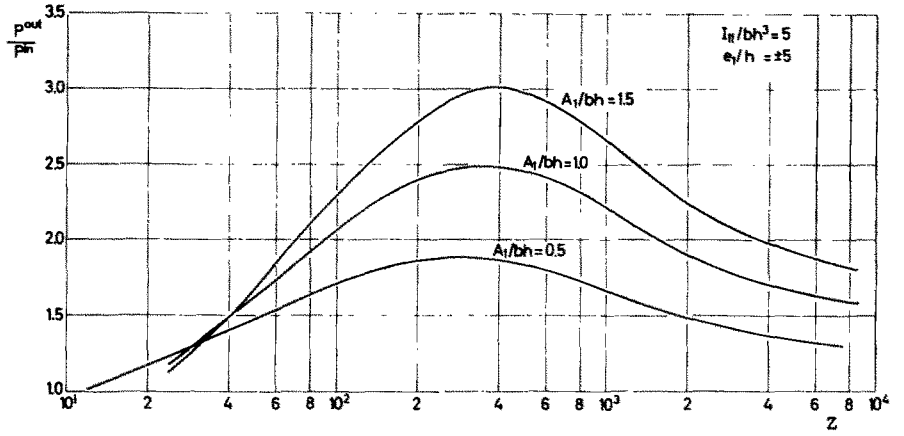

FIG. 8. Influence of (A_1/bh) on eccentricity effect.

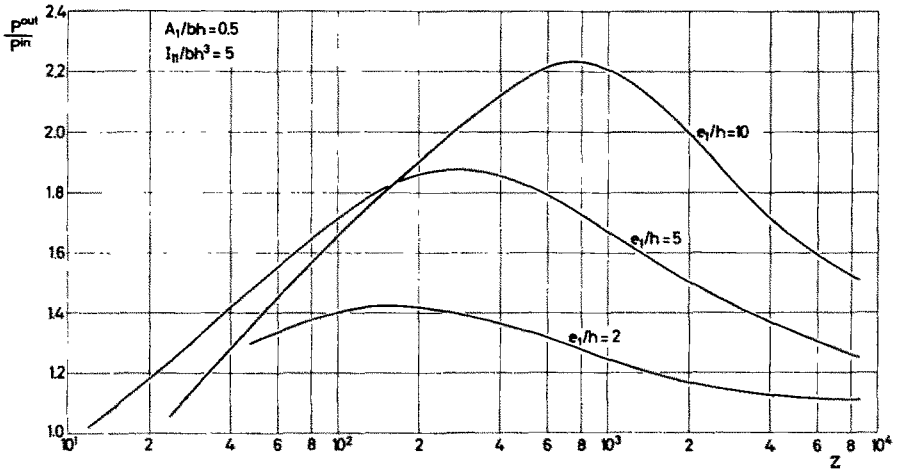

FIG. 9. Influence of magnitude of $|e_1/h|$ on eccentricity effect.

The torsional rigidity of the stiffener η_{t1} has been neglected in the preceding discussion. For the case of ring stiffened cylindrical shells under torsion [21], the influence of the torsional rigidity was found to be appreciable for certain geometries. Hence the influence of η_{t1} on the buckling load is investigated here in Fig. 10. The range of values of $\eta_{t1} = 5$ to $\eta_{t1} = 40$ considered, is realistic and represents fairly large stringers with open and closed sections. The influence of the torsional rigidity of the stiffeners is larger for inside stringers and is important here, in the case of axial compression, even for large Z that represent

practical design dimensions. For example, for $\eta_{t1} = 10$–20, increases of 25–50% in buckling loads are found in Fig. 10, or increases of up to 25% in Table 3, where the theoretical calculations are correlated with the experimental results of [9].

TABLE 1. ECCENTRICITY EFFECT FOR CYLINDRICAL SHELLS WITH HEAVY STRINGERS

L/R	R/h	A_1/bh	I_{11}/ah^3	$\lvert e_1/h\rvert$	inside (+)		outside (−)		λ^-/λ^+
					λ^+	t	λ^-	t	
1·0	250	1·5	5	7	8432	7	23,380	10	2·891
	500				10,150	10	33,900	13	3·340
	1000				15,180	13	50,060	15	3·299
1·0	250	1·5	5	10	14,780	7	39,700	10	2·686
	500				15,730	9	51,720	13	3·288
	1000				19,240	12	70,690	16	3·674
2·0	500	1·5	5	10	7471	8	25,890	9	3·465
		3·0			7597	7	39,650	10	5·220
		5·0			13,970	10	81,770	12	5·852

TABLE 2. RING-STIFFENED CYLINDERS UNDER AXIAL COMPRESSION
AXISYMMETRIC AND ASYMMETRIC

($L/R = 0{\cdot}5$ $\nu = 0{\cdot}3$)

R/h	A_2/ah	I_{22}/ah^3	e_2/h	inside rings (+)			outside rings (−)			λ^+/λ_{UNS}	λ^-/λ_{UNS}
				λ^+	t	n	λ^-	t	n		
50	0·5	5	5	718·4	3	2	809·4	0*	2	1·086	1·223
100				1420	4	3	1619		3	1·072	1·222
250				3578	6	5	4048		5	1·066	1·206
500				7063	8	6	8094		6	1·062	1·211
1000				14,050	11	9	16,190		9	1·062	1·224
2000				28,080	16	13	32,380		13	1·062	1·225
250	0·5	2	0	4016	5	5	†			1·196	
		5		4033	3	5				1·201	
		20		4044	2	5				1·205	
		40		4046	1	5				1·205	
		200		4048	0	5				1·206	
250	0·5	5	0·5	3994	4	5	4048	0	5	1·190	1·206
		2	1	3854	7	5	4048		5	1·148	1·206
		40	1	4030	2	5	4048		5	1·200	1·206

* $t = 0$ means axisymmetric buckling.
† results for outside and inside rings are the same because $e_2 = 0$.

The buckling loads of the stiffened and unstiffened cylindrical shells compared in the discussion were calculated by linear small deflection theory. For unstiffened cylinders under axial compression, experimental results are well known to be much below the buckling loads computed with linear theory. Closely stiffened shells, on the other hand show good agreement between experiment and linear theory, see for example [9, 32, 33] and Section 5 of [29], and can therefore be adequately analysed by linear theory.

TABLE 3. COMPARISON OF THEORETICAL AND CARD'S EXPERIMENTAL RESULTS

No.	Shell geometry		Stringer geometry				P (kips)		P (kips) Test Ref. [9]	P obtained by [14] (kips)	
	L/R	R/h	A_1/bh	I_{11}/bh^3	e_1/h	η_{r1}	simply supp.	clamped		simply supp.	clamped ends
1	3·98	338	1·03	9·79	−5·83	0	62·57*(6)	113·8 (7)	112·6 (6)	61·93 (6)	114·5 (7)
						17	71·61 (6)	128·0 (7)			
2	3·98	345	1·06	10·5	5·96	0	35·22 (7)	47·96 (8)	48·0 (6)	34·98 (7)	47·76 (8)
						18·2	43·15 (5)	62·82 (7)			
3	2·49	347	1·07	10·8	−6	0	71·0 (7)	142·4 (9)	127·2 (7)	70·8 (7)	143·0 (9)
						18·6	83·35 (7)	163·8 (8)			
4	2·49	341	1·05	10·1	5·89	0	36·64 (7)	63·85 (8)	61·6 (6)	35·4 (7)	61·98 (8)
						17·6	45·93 (6)	77·81 (7)			

* The number in brackets is equal to the number of circumferential waves.

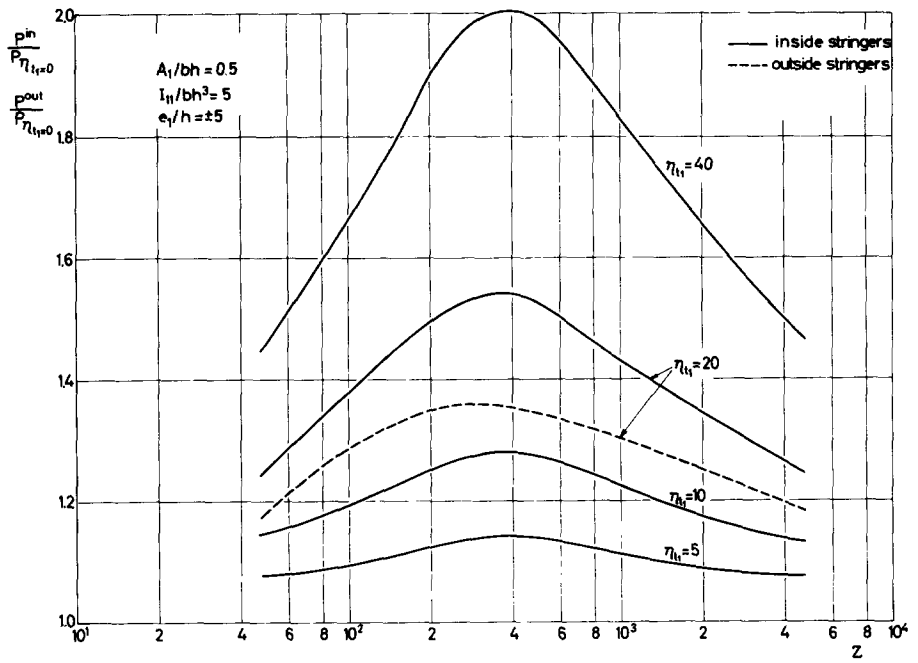

FIG. 10. Influence of torsional rigidity of stringers on stiffening of shell.

A recent study of the imperfection sensitivity of eccentrically stiffened cylindrical shells [34] points out that imperfection sensitivity might invalidate the predictions of linear theory over a substantial range of Z, especially in the case of stringer stiffened shells. Experiments to date [9, 33] that cover Z values of 160–5000 and (R/h) values of 300–700, do not seem to confirm this fear. The authors feel, therefore, that for closely and fairly heavily stiffened shells of practical dimensions linear theory is valid.

Hence, if one wants a clearer picture of the effectiveness of stringers as stiffeners of axially compressed cylindrical shells, one may correct the buckling loads of the unstiffened shells, considered in Fig. 6, according to experimental results, whereas linear theory is considered valid for stiffened shells. An empirical formula for this correction is proposed in [35]. According to Fig. 3 of the same reference, the correction, equations (26) below, is conservative in comparison with test results of 14 different investigators. The proposed correction factor is

$$K = (P_{cor}/P_{UNS}) \simeq 1 - 0{\cdot}901\left\{1 - \exp\left[-\tfrac{1}{16}\sqrt{\left(\frac{R}{h}\right)}\right]\right\} \tag{26}$$

The influence of the length of the shell on K has not been explored in great detail in [35] or earlier investigations. Preliminary experimental studies discussed in [35] indicate that the length has only a small effect on the correction factor K of equation (26), and length is therefore not included in the empirical correction employed here.

Figure 11 compares the buckling load of axially compressed stringer-stiffened shells with that of equivalently thickened ones (the equivalence refers here to equal weight). The buckling loads of the equivalently thickened unstiffened shells are corrected according

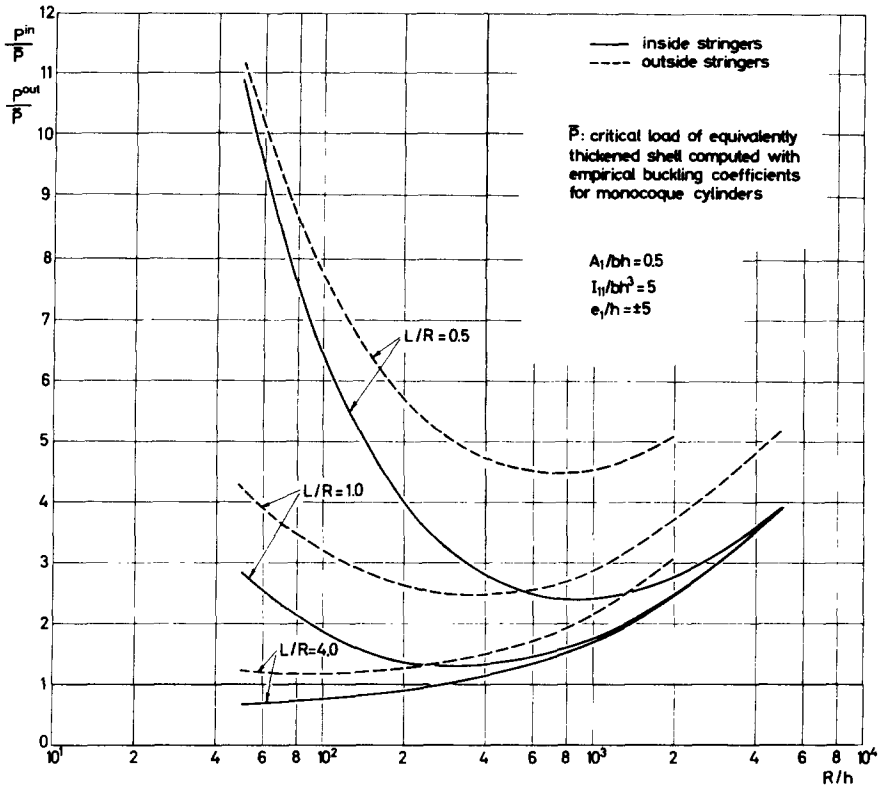

FIG. 11. Corrected structural efficiency of stringer stiffened cylindrical shell with simple supports.

to equation (26). Hence

$$(P^{out}/\bar{P}) = (P^{out}/KP_{UNS.EQ.}) \tag{27}$$

and similarly for P^{in}. Note that $\bar{P}$ is the critical load of an equivalently thickened shell corrected by equation (26). Figure 11 is therefore a "corrected" restatement of Fig. 6 for simple supports. However, here the plot is not versus Z as in Fig. 6, but versus (R/h), with (L/R) as an additional parameter, since the correction factor K depends on (R/h) and not on Z. The minima in $(P^{out}/\bar{P})$, or $(P^{in}/\bar{P})$, observed in Fig. 11, are due to different rates of decrease of K and $(P^{out}/P_{UNS.EQ.})$, with (R/h). It is seen that outside stiffening is always better than equivalent thickening of shell, irrespective of shell geometry. For inside stringers there seems to be a range of (L/R) and (R/h) for which equivalent thickening is preferable.

In Fig. 12 the influence of stiffener cross-sectional area on the "corrected" structural efficiency is studied. The cross-sectional area of the stringer is chosen as a parameter to show that increase in stiffener area may be detrimental to structural efficiency, and may mean such a weight increase that equivalent thickening is better even after the empirical correction is applied.

In Table 3 the experimental buckling loads obtained by Card [9] are compared with values calculated for classical simple supports, equation (6), and for classical clamped ends, equations (18). Only the 4 integrally machined cylinders are compared. Theoretical values without η_{t1} and with η_{t1} are given in Table 3 and again neglect of the torsional rigidity η_{t1}

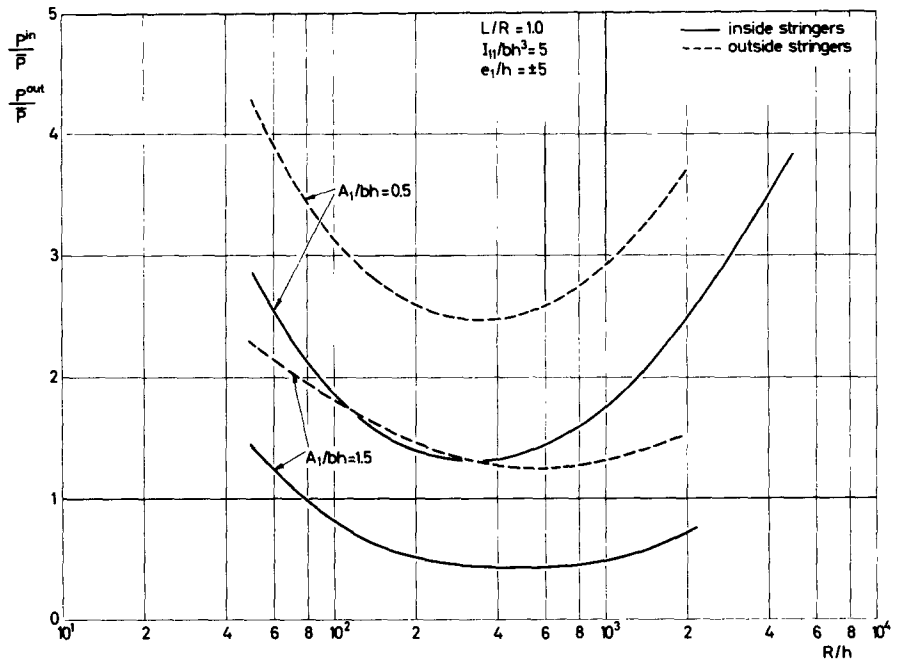

FIG. 12. Influence of stiffener cross-sectional area on structural efficiency of simply supported shell.

is not justified here. The experimental buckling loads fall between the computed simple supports and clamped end values, slightly closer to the clamped end values. Since the test end conditions, flat ends between platens of a testing machine, are nearer to clamped ends than to simple supports, the correlation is satisfactory. For comparison, the theoretical buckling loads computed by Hedgepeth and Hall [14] for Card's test cylinders are also presented in Table 3. Hedgepeth and Hall neglect the torsional rigidity and hence their values are similar to those computed here with $\eta_{t1} = 0$. They also neglect in their theory [14] the bending and twisting stiffness of the skin, but in the case of Card's cylinders this neglect is permissible. The small differences are mainly due to slightly different interpretations of the geometries presented in [9].

A more general comparison between the theory of Hedgepeth and Hall [14] and that employed here, which was originally derived in [5], may be useful. In [14] an attempt is made to simplify the theory by neglect of "unimportant" stiffness contributions in order to facilitate deduction of general conclusions. For stringer stiffened shells the bending and twisting stiffness of the skin as well as the torsional rigidity of the stringers are neglected. Hence, for simple supports, one can summarize the comparison with the present theory by the following relation

$$P = P_{HH} + [(2/n^2\beta^2)(n^2\beta^2 + t^2)^2 + 2t^2\eta_{t1}](\pi D/R) \tag{28}$$

where P is the critical axial load obtained here and P_{HH} is the critical load obtained in [14]. The importance of the torsional rigidity has already been discussed. The first term in the square brackets of equation (28) is important only when t is large. Hence neglect of this term is often justified, but sometimes considerable errors may result. For example, in a

typical shell with $(R/h) = 500$, $(L/R) = 1{\cdot}0$, $(e_1/h) = 5$, $(A_1/bh) = 1{\cdot}5$ and $(I_{11}/bh^3) = 5$, the buckling load is 40% higher when the term $(2/n^2\beta^2)(n^2\beta^2 + t^2)^2$ is included.

CONCLUSIONS

The results of the calculations for 350 typical shells under axial compression show that the behavior of the eccentricity effect depends very strongly on the geometry of the shell while the geometry of the stiffeners only influences its magnitude. For all practical geometries outside stringers yield higher buckling loads than inside ones. The eccentricity effect has a pronounced maximum which occurs for values of Z which are common in aerospace practice. The behavior of the eccentricity effect for shells with clamped ends is very similar to that for simply supported shells. Rings when alone, are much less efficient as stiffeners. With inside rings the buckling load is reduced by the eccentricity, whereas with outside rings the axisymmetric pattern, that is not influenced by eccentricity dominates.

Acknowledgements—The authors would like to thank Mr. R. Haftka for checking of derivations, Mr. E. Glinert for assistance with the programming, Mrs. J. Stern for assistance with the computations and the staff of the Technion Computing Center for their valuable help.

REFERENCES

[1] A. VAN DER NEUT, The general instability of stiffened cylindrical shells under axial compression, Report S.314, National Luchtvaartlaboratorium, Amsterdam, Report and Transactions, **13,** S.57 (1947).
[2] L. B. WILSON, Deformation under uniform pressure of a circular cylindrical shell supported by equally spaced circular ring frames. Report R.337C, Naval Construction Research Establishment, St. Leonard's Hill, Dunfermline, Fife, December 1956.
[3] S. KENDRICK, The buckling under external pressure of circular cylindrical shells with evenly spaced equal strength circular ring frames. Report R.211, Naval Construction Research Establishment, Dunfermline, Fife, February 1953.
[4] G. CZERWENKA, Untersuchungen von dünnen kurzen Zylindern die durch Ringkleinstprofile enger und mittlerer Teilung verstärkt sind und unter Manteldruck stehen. *Z. Flugwiss.* **10,** 163 (1961).
[5] M. BARUCH and J. SINGER, Effect of eccentricity of stiffeners on the general instability of stiffened cylindrical shells under hydrostatic pressure. *J. mech. Engng Sci.* **5,** 23 (1963).
[6] M. BARUCH and J. SINGER, General instability of stiffened circular conical shells under hydrostatic pressure. *Aeronaut. Q.* **26,** 187 (1965). Also Technion Research and Development Foundation, Haifa, Israel, TAE Report 28, July 1963.
[7] M. BARUCH, J. SINGER and O. HARARI, General instability of conical shells with non-uniformly spaced stiffeners under hydrostatic pressure, Proc. 7th Israel Annual Conf. on Aviation and Astronautics, *Israel Jnl Technol.* **3,** 62 (1965). Also Technion Research and Development Foundation, Haifa, Israel, TAE Report 37, December 1964.
[8] D. S. HOUGHTON and A. S. L. CHAN, Design of a pressurised missile body. *Aircr. Engng* **32,** 320 (1960).
[9] M. F. CARD, Preliminary results of compression tests on cylinders with eccentric longitudinal stiffeners. NASA TM X-1004, September 1964.
[10] A. J. DE LUZIO, C. E. STUHLMAN and B. O. ALMROTH, Influence of stiffeners eccentricity and end moment on the stability of cylinders in compression. Presented at the *AIAA 6th Structures and Materials Conf.*, Palm Springs, April 1965.
[11] H. D. GARKISCH, B. GEIER and P. SEGGELKE, Beulversuche an längsversteiften Zylinderschalen. To be published as a Deutsche Luft- und Raumfahrt, Forschungsbericht.
[12] A. VAN DER NEUT, General instability of orthogonally stiffened cylindrical shells. Collected Papers on Instability of Shell Structures—1962, NASA TN D-1510, 309, December 1962.
[13] J. M. HEDGEPETH, Design of stiffened cylinders in axial compression. Collected Papers on Instability of Shell Structures—1962, NASA TN D-1510, 77, December 1962.
[14] J. M. HEDGEPETH and D. B. HALL, Stability of stiffened cylinders. *AIAA Jnl* **3,** 2275 (1965).

[15] J. A. McElman, M. M. Mikulas and M. Stein, Static and dynamic effects of eccentric stiffening of plates and cylindrical shells. Presented at the *2nd AIAA Annual Meeting and Technical Display*, San Francisco, July 1965.
[16] D. L. Block, M. F. Card and M. M. Mikulas, Buckling of eccentrically stiffened orthotropic cylinders. NASA TN D-2960, August 1965.
[17] B. Geier and P. Seggelke, Das Beulverhalten versteifter Zylinderschalen, Teil 2, Beullasten bei axialsymmetrischer Belastung, To be published in *Z. Flugwiss.*
[18] R. F. Crawford, Effects of asymmetric stiffening on buckling of shells. Presented at the *2nd AIAA Annual Meeting and Technical Display*, San Francisco, July 1965.
[19] W. Thielemann and M. Esslinger, Über den Einfluss der Exzentrizität von Längssteifen auf die axiale Beullast dünnwandiger Kreiszylinderschalen. *Stahlbau* **34**, 332 (1965).
[20] J. Singer, M. Baruch and O. Harari, Further remarks on the effect of eccentricity of stiffeners on the general instability of stiffened cylindrical shells, *J. mech. Engng. Sci.* **8**, 363 (1966). Also Technion Research and Development Foundation, Haifa, Israel, TAE Report 42, August 1965.
[21] M. Baruch, J. Singer and T. Weller, Effect of eccentricity of stiffeners on the general instability of stiffened cylindrical shells under torsion. Proc. 8th Israel Annual Conference on Aviation and Astronautics. *Israel Jnl. Technol.* **4**, 144 (1966). Also Technion Research and Development Foundation, Haifa, Israel, TAE Report 43, August 1965.
[22] S. B. Batdorf, Simplified method of elastic stability analysis for thin cylindrical shells. NACA Report 874, 1947.
[23] N. J. Hoff, Low buckling stresses of axially compressed circular cylindrical shells. *J. appl. Mech.* **32**, 533 (1965).
[24] N. J. Hoff and T. C. Soong, Buckling of circular cylindrical shells in axial compression. *Int. J. mech. Sci.* **7**, 489 (1965).
[25] B. O. Almroth, Influence of edge conditions on the stability of axially compressed cylindrical shells, *AIAA Jnl* **4**, 134 (1966).
[26] W. Thielemann and M. Esslinger, Einfluss der Randbedingungen auf die Beullast von Kreiszylinderschalen. *Stahlbau* **33**, 353 (1964).
[27] F. C. Card and R. M. Jones, Experimental and theoretical results for buckling of eccentrically stiffened cylinders. NASA TN D-3639, October 1966.
[28] J. Singer, M. Baruch and O. Harari, On the stability of eccentrically stiffened cylindrical shells under axial compression. Technion Research and Development Foundation, Haifa, Israel, TAE Report 44, December 1965.
[29] J. Singer, A. Berkovits, T. Weller, O. Ishai, M. Baruch and O. Harari, Experimental and theoretical studies on buckling of conical and cylindrical shells under combined loading. TAE Report 48, Technion Research and Development Foundation, Haifa, Israel, June 1966.
[30] S. P. Timoshenko and J. M. Gere, *Theory of Elastic Stability*. McGraw-Hill (1961).
[31] W. F. Thielemann, New developments in the nonlinear theories of the buckling of thin cylindrical shells. *Aeronautics and Astronautics, Proc. of Durand Centennial Conf.*, Stanford 1959, p. 76. Pergamon Press (1960).
[32] G. Gerard, Elastic and plastic stability of orthotropic cylinders. Collected Papers on Instability of Shell Structures—1962, NASA TN D-1510, p. 277, December 1962.
[33] R. Milligan, G. Gerard, and C. Lakshmikantham, General instability of orthotropically stiffened cylinders in axial compression. *AIAA Jnl* **4**, 1906 (1966).
[34] J. W. Hutchinson and J. C. Amazigo, Imperfection-sensitivity of eccentrically stiffened cylindrical shells. Report SM-10, Harvard University, Cambridge, Mass, April 1966.
[35] V. I. Weingarten, E. J. Morgan and P. Seide, Elastic stability of thin-walled cylindrical and conical shells under Axial compression, *AIAA Jnl* **3**, 500 (1965).

(*Received* 4 *May* 1966; *revised* 19 *January* 1967)

Résumé—L'effet de l'excentricité des pièces de support sur la charge critique est étudiée pour des coquilles cylindriques sous compression axiale. Le support simple classique et les conditions d'extrémité de serrage classique sont considérées. Une explication physique détaillée des causes de l'effet d'excentricité est proposée et vérifiée par des calculs portant sur 350 coquilles typiques. Comme dans le cas due flambement sous l'effet de la torsion et de la pression hydrostatique le comportement de l'effet d'excentricité dans le cas de la compression axiale dépend aussi très fortement de la géométrie de la coquille, représentée par le paramètre de Batdorf. D'autre part la géométrie des pièces de support n'influence que sa grandeur. Pour une valeur Z très réduite, un renversement de l'effet d'excentricité a lieu, mais pour des dimensions pratiques les longerons extérieurs raidissent la coquille

plus que les longerons intérieurs. L'effet d'excentricité a un maximum prononcé pour les valeurs pratiques de Z. Le comportement de l'effet d'excentricité est très semblable pour des coquilles à serrage et pour des coquilles simplement supportées. Les effets d'excentricité des pièces de support annulaires sont aussi considérés.

Zusammenfassung—Die Einwirkung der Versteifungs-Exzentrizität auf die kritische Belastung wird für zylindrische Schalen unter Längsbelastung untersucht. Klassische Bedingungen der einfachen Stütze wie auch eingespannte Enden werden ermittelt. Eine genaue physikalische Erklärung der Ursachen des Exzentrizitätseffekts wird vorgeschlagen und durch Berechnung von 350 typischen Schalen bestätigt.

Wie im Falle des Beulens bei hydrostatischem Druck und Torsion hängt des Verhalten des Exzentrizitätseffekts bei Längsbelastung sehr von der Gestalt der Schale ab, diese wird durch den Batdorf'schen Parameter dargestellt. Andererseits beeinflusst die Gestalt der Versteifungen nur deren Grösse. Bei geringen Z-Werten erfolgt Inversion des Exzentrizitätseffekts, aber praktisch versteifen Aussenträger die Schale mehr als Innenträger. Der Maximalwert des Exzentrizitätseffekt erscheint bei praktischen Z-Werten. Der Exzentrizitätseffekt ist für eingespannte sowie für einfach gestützte Schalen sehr ähnlich. Der Einfluss ringförmiger Versteifungen wird auch untersucht.

Абстракт—Рассуждается эффект эксцентричности ребер жесткости на критическую нагрузку в цилиндрических оболочках сжатых осевым давлением. Рассматриваются классические граничные условия свободного и закрепленного края. Предлагается детальное физическое выяснение причин эффекта эксцентричности, проверенное и исследуя 350 типичных оболочек.

Так как в случае выпучивания гидростатическим давлемием и кручением, поведение эффекта эксцентритета в случае осевого давления также зависят в большой степени от геометрии оболочки, представленной параметром Батдорфа. С другой стороны геометрия ребер жесткости влияет только на их величину. При очень малом Z, происходит инверсия эффекта эксцентричности, но для практических расчетов, внешние ребра жесткости, всегда усиливают оболочку больше чем внутрениие. Эффект эксцентричности имеет определенный максимум при практических значениях Z. Поведение эффекта эксцентритета очень подобно для закрепленных и свободно опертых оболочек. Рассмотрен также эффект эксцентритета при наличии кругообразных ребер жесткости.